Vibrational Spectroscopy 55 (2011) 183–187

Contents lists available at ScienceDirect

Vibrational Spectroscopy

journal homepage: www.elsevier.com/locate/vibspec

Alkali metal intercalated titanate nanotubes: A vibrational spectroscopy study

Bartolomeu C. Viana [a], Odair P. Ferreira [b], Antonio G. Souza Filho [c,b,*], Angel A. Hidalgo [a], Josué Mendes Filho [c], Oswaldo L. Alves [b]

[a] Departamento de Física, Universidade Federal do Piauí – UFPI, P.O. Box CEP 64049-550, Teresina, PI, Brazil
[b] LQES – Laboratório de Química do Estado Sólido, Instituto de Química, Universidade Estadual de Campinas – UNICAMP, P.O. Box 6154, CEP 13083-970, Campinas, SP, Brazil
[c] Departamento de Física, Universidade Federal do Ceará – UFC, P.O. Box 6030, CEP 60455-900, Fortaleza, CE, Brazil

ARTICLE INFO

Article history:
Received 3 October 2010
Received in revised form 1 November 2010
Accepted 18 November 2010
Available online 1 December 2010

Keywords:
Titanate nanotubes
Raman spectroscopy
Inorganic nanotubes

ABSTRACT

Alkali metal (Li^+, Na^+, K^+) intercalated titanate nanotubes have been studied by vibrational spectroscopy (Raman and FT-infrared), X-ray diffraction, and electron microscopy. The vibrational spectroscopic data shown that the most affected vibrational mode is that related to Ti–O bond whose oxygen is not shared among the TiO_6 units of the framework structure. A correlation between vibrational frequency shifts and intercalated metal was found, thus showing that vibrational spectroscopy is very useful for probing metal intercalated titanate nanotubes. Our results provide good evidences that the structure of titanate layers in titanate nanotube, a subject of long debate in the literature, is similar to trititanates (like $Na_2Ti_3O_7$).

1. Introduction

Elongated TiO_2 based nanostructures such as nanotubes and nanoribbons exhibit some properties that differ from their bulk counterparts [1,2]. In particular, alkali titanate nanotubes have received a great deal of attention, in part because these nanomaterials have a large surface area that leads to a wide variety of applications. Alkali titanates, usually possessing a layered or tunnel-type structure, have been the subject of extensive investigation and may be applied to photocatalysis, photoluminescence and dye-sensitized solar cells due to their excellent ion-exchange ability and photocatalytic activities [2–8].

Alkali titanate nanotubes have mostly been prepared through hydrothermal treatment of TiO_2 powders in aqueous NaOH solutions. This method is very simple, inexpensive and efficient for obtaining samples with sharp morphological distribution [9]. However, a debate has been established in the literature regarding the composition and atomic structure of the titanate nanotubes [7,10–14]. Several models have been proposed to the composition and atomic structure of titanate nanotubes [9,11–21]. Sodium trititanate ($Na_2Ti_3O_7$) is regarded as one of the candidates for a similar atomic structure observed in the walls of titanate nanotubes [14,18]. Different groups agree that hydrothermal treatment induces the breaking of chemical bonds of the three-dimensional TiO_2 structure by highly concentrated aqueous solution of NaOH. After that, there is the formation of intermediate titanate sheets and the nanotubes are formed by rolling up of these intermediate sheets, thus forming a scroll-like geometry [20].

Sodium trititanate nanotubes have a structure in which TiO_6 octahedra join each other to form layers carrying negative electrical charges and exchangeable sodium cations between the layers [22]. The optical properties of titanate nanotubes can be modified in a controlled way using ion exchange reactions (or intercalation) of other metals [6,16,23,24]. Such methodology is suitable for probing changes in the chemical bonds of the structure, thus, allowing one to further understand the titanate nanotube composition and structure [25,26].

In this work, we report a study on the structural and vibrational properties of the sodium titanate nanotubes prepared by hydrothermal method (Na^+ intercalated nanotubes) and submitted to ion exchange reactions for obtaining Li^+ and K^+ intercalated titanate nanotubes. By analyzing the vibrational data obtained and based on the information available in the literature for both nanotubes and bulk titanates [22,25,27,28], we have studied the ion intercalation effects in the titanate nanotube structure. The intercalation affects the vibrational properties of the titanate nanotubes to a great extent. The wavenumber shifts for some Ti–O vibrations due to intercalation by different metals are discussed and the correlation with the atomic bonds is made.

* Corresponding author at: Departamento de Física, Universidade Federal do Ceará – UFC, P.O. Box 6030, CEP 60455-900, Fortaleza, CE, Brazil. Tel.: +55 85 33669008; fax: +55 85 33669450.
E-mail addresses: agsf@fisica.ufc.br, souzafilhoag@gmail.com (A.G.S. Filho).

0924-2031 © 2010 Elsevier B.V. Open access under the Elsevier OA license.
doi:10.1016/j.vibspec.2010.11.007

2. Experimental

All chemicals (reagent grade, Aldrich, Merck, or Baker Analyzed) were used as received, without further purification. All solutions were prepared with deionized water.

2.1. Preparation of titanate nanotubes

Sodium titanate nanotubes (Na-TiNT) were prepared as described previously by Ferreira et al. [18]. In a typical synthesis, 2.00 g (25.0 mmol) of TiO_2 (anatase) were suspended in 60 mL of 10 mol L^{-1} aqueous NaOH solution for 30 min in a beaker. The white suspension formed was transferred to a 90 mL Teflon-lined stainless steel autoclave and kept at 165 ± 5 °C for 170 h. After that, the autoclave was naturally cooled down to room temperature and the obtained sample was subsequently filtered and washed several times with deionized water until pH 11–12. The sample was dried at 60 ± 10 °C for 24 h.

2.2. Ion exchange reactions of titanate nanotubes

We used Na-TiNTs for exchange reactions because the methodology we used in the synthesis generates Na intercalated TiNTs and they are suitable for exchange reactions without going through the protonation process.

Metal ion (Li^+ and K^+) exchange reactions were carried out by suspending 100 mg of Na-TiNTs in 100 mL of 0.05 mol L^{-1} aqueous solutions of $LiNO_3$ and KNO_3, respectively. The suspension was left under magnetic stirring for 24 h at room temperature (at about 25 °C). The solid product was isolated by centrifugation under 3000 rpm and it was washed several times with deionized water aiming to remove the remaining soluble ions from the precursor. The solid product was dried under vacuum conditions during 6 h to obtain the metal intercalated titanate nanotubes (Li-TiNT and K-TiNT).

2.3. Characterization

Fourier transform infrared (FT-IR) spectra were recorded using the KBr pellet (transmission) and ATR FT-IR technique on a Bomen FTLA 2000 and a Bruker Vertex 70 spectrometer, respectively. A total of 64 scans and a resolution of 4 cm^{-1} were used for getting spectra with good signal to noise ratios. The Raman spectroscopy experiments were performed on a Jobin-Yvon T6400 spectrometer equipped with an Olympus microscope. A 532 nm laser Verdi V-5 from Coherent was used for exciting the Raman spectra. Low laser power density was used in order to avoid sample overheating. A spectral resolution of 1 cm^{-1} was used and measurements were performed using a backscattering geometry. X-ray powder diffraction (XRD) patterns were obtained with a Shimadzu XRD7000 diffractometer, using Cu Kα (λ = 1.5406 Å) radiation operating with 30 mA and 40 kV. A scan rate of 1 min^{-1} was used. Transmission electron microscopy (TEM) images were obtained using a FEI-Tecnai G^2S-Twin setup both operating with 200 kV. The TEM samples were prepared by dropping an aqueous suspension of the sample powder on a holey carbon-coated copper grid and letting the water evaporate at room temperature.

3. Results and discussion

In order to study the vibrational properties of titanate nanostructures we first review the group theory analysis of vibrations for $Na_2Ti_3O_7$ bulk structures. Bulk $Na_2Ti_3O_7$ at room temperature exhibits a lamellar structure (monoclinic, space group $P2_1/m$ ($C_{2h}{}^2$)) with two formulas per unit cell ($Z = 2$). Group theory predicts that $Na_2Ti_3O_7$ would exhibit 69 vibrational modes distributed among the irreducible representations as follows: 24 A_g + 11 A_u + 12 B_g + 22 B_u. Both A_g (A_u) and B_g (B_u) are Raman (IR) active representations. Before discussing the vibrational data of alkali metal intercalated titanate nanotubes, we should mention that these materials have a scroll-like structure and it is not appropriate to apply standard factor group analysis, because there is no radial symmetry. Therefore, the analysis will consider the atomic vibrations in comparing with $Na_2Ti_3O_7$ without specifying the mode symmetry.

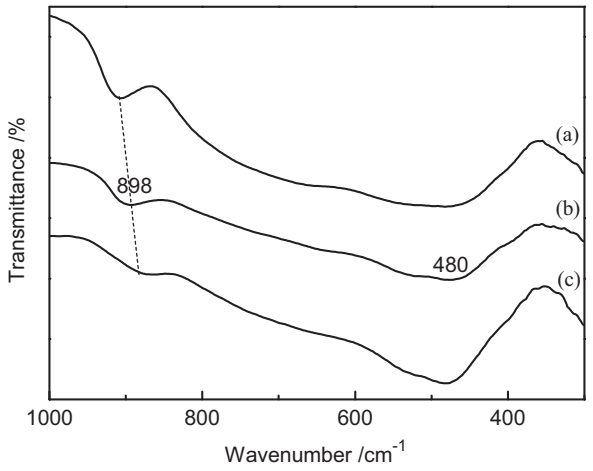

Fig. 1. FT-IR absorption spectra of (a) K^+, (b) Na^+ and (c) Li^+ intercalated titanate nanotubes. We observe the shift of the mode at 898 cm^{-1} in K-TiNT and Li-TiNT.

In Fig. 1, we show the FT-IR spectra for alkali–metal intercalated titanate nanotubes. It is clear from the spectral features that the tubular morphology is preserved after promoting the ionic exchange reactions. However, the energy of some vibrational modes depends on the intercalated ion. The highest energy mode (898 cm^{-1}) which is assigned to the stretching of the Ti–O bonds (from distorted TiO_6 octahedron) whose oxygen is unshared, as described in Refs. [6,14,18,29], was affected by the different ions, and the wavenumber of this mode depends on intercalated ions as follows: $\nu_{K^+} > \nu_{Na^+} > \nu_{Li^+}$. The modes at about 480 and 540 cm^{-1} exhibit a different behavior getting a slight hardening, i.e., $\nu_{K^+} < \nu_{Na^+} < \nu_{Li^+}$. The $\Delta\nu$ for ν_{Ti-O} (898 cm^{-1}) is about 29 cm^{-1}, being much larger than $\Delta\nu$ for the 480 cm^{-1} mode which is about 4 cm^{-1} (close to the applied spectral resolution). The changes in the energy of these vibrational modes can be associated with the different intercalated ions in the nanotube walls. Although the ions have the same positive charge, it is expected that they would distort the electronic cloud of the oxygen atoms from octahedra (nanotube walls) in different ways. As a consequence, the charge redistribution renormalizes the Ti–O bond strength, thus changing the vibrational energies. Due to the different electronegativities, it is expected that Li would transfer more charge to the layers, thus softening the Ti–O bond as compared with Na^+ and K^+. The modes at about 480 cm^{-1} are practically unchanged, because these modes can be assigned as bending modes of TiO_6 octahedra (mainly involving shared oxygen atoms) and they do not interact directly with intercalated ions. The ATR FT-IR spectra for alkali–metal intercalated titanate nanotubes (see the Supplementary material) were recorded to investigate the possible effects of KBr pelleting on the nanotubes vibrations. However, we did not observe any difference in the ATR FT-IR spectra as compared with transmission FT-IR spectra (KBr pellets).

The Raman spectra of alkali–metal-intercalated titanate nanotubes are shown in Fig. 2. According to previous works, the bands at about 160 and 196 cm^{-1} are attributed to the Na. . .O–Ti bending modes. The bands at about 280, 454, and 663 cm^{-1} are assigned

Table 1
Ionic radii (pm) of Li^+, Na^+ and K^+ [33], and highest FT-IR and Raman wavenumbers and Raman Lattice modes for intercalated nanotubes.

Intercalated ion	Radii (pm)	FT-IR (cm^{-1}) (Ti–O)	Raman (cm^{-1}) (Ti–O)	Raman Lattice modes (cm^{-1})
Li+	59	880	893	187
Na+	102	898	905	196
K+	138	909	917	189

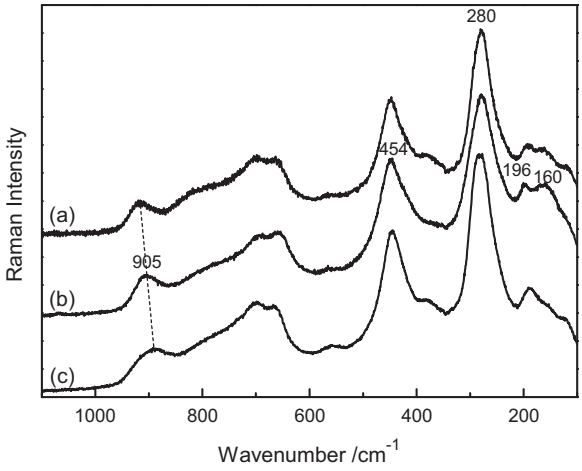

Fig. 2. Raman spectra of (a) K^+, (b) Na^+, and (c) Li^+ intercalated titanate nanotubes. We observe the shift of the mode at 905 cm^{-1} in K-TiNT and Li-TiNT.

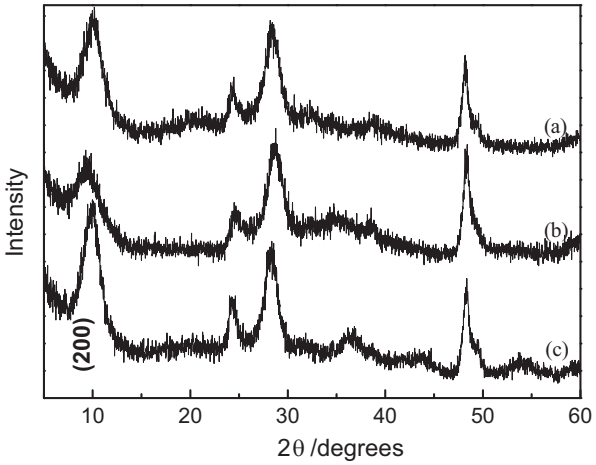

Fig. 3. X-ray diffraction patterns of (a) K^+, (b) Na^+ and (c) Li^+ intercalated titanate nanotubes. The diffraction plane (2 0 0) of the TiNT was identified in the pattern.

to the Ti–O–Ti stretching in edge-shared TiO_6 and the bands at about 905 cm^{-1} represent the stretching vibration of the short Ti–O bonds in distorted TiO_6 unit [6,9,25,29,30]. Similarly to FT-IR spectra, we observe that the highest energy mode has its wavenumber considerably affected by the intercalated ionic species. The $\Delta\nu$ for the highest Raman mode is about 24 cm^{-1} (893 cm^{-1} for Li-TiNT and 917 cm^{-1} for K-TiNT), in accordance with FT-IR results. Some lower energy modes (about 655 and 196 cm^{-1}) also change their wavenumbers but the changes are not much pronounced, the shifts being about 7–9 cm^{-1}, which is considerably smaller than the bandwidth. Furthermore, different degrees of structural disorder can lead to such shifts. For both FT-IR and Raman, the most affected mode is that related to Ti–O bond whose oxygen is not shared among the TiO_6 units (at the corner of the TiO_6 octahedral slab). This is a good evidence that the structure of sodium titanate layers is similar to sodium trititanate, $Na_2Ti_3O_7$, since that structure has these Ti–O terminal bonds where the oxygen is unshared [6,14,18,31]. Lepidocrocite-type [21] and $H_2Ti_2O_5{\cdot}H_2O$ [20] are other structures proposed to titanate nanotubes, but they have no such Ti–O terminal bonds.

In order to better understand the structure–vibrational spectrum relationship, X-ray diffraction experiments were performed which provide information about the interlayer distance as well as about the crystalline order within the layers. Similar to what vibrational spectra pointed out, the X-ray diffraction data (Fig. 3) indicated that both the structure and the morphology of ion-intercalated titanate nanotubes are preserved. The ion intercalation affected the diagonal planes of the nanotube structure at about 36° [15]. The peak at about 10° (200 plane) is related to interlayer distance [32] and we observed, trough 2θ position, in these measurements that Na^+ intercalated nanotubes present the largest interlayer distance for the intercalated ions studied here. The interlayer distances were estimated by XRD and they were obtained 0.89, 0.90 and 0.95 nm for K^+, Li^+ and Na^+ intercalated titanate nanotubes, respectively. The XRD data revealed the following sequence for interlayer distance: d(Na-TiNT) > d(Li-TiNT) > d(K-TiNT) as schematically show in Fig. 4. The relation d(Na-TiNT) > d(Li-TiNT) is expected since the ionic radius of Li^+ is smaller than that of Na^+. The ionic radii for Li^+, Na^+ and K^+ are listed in Table 1, according to Shannon and Prewitt [33]. However, the smallest value observed in the K^+ intercalated TiNTs for

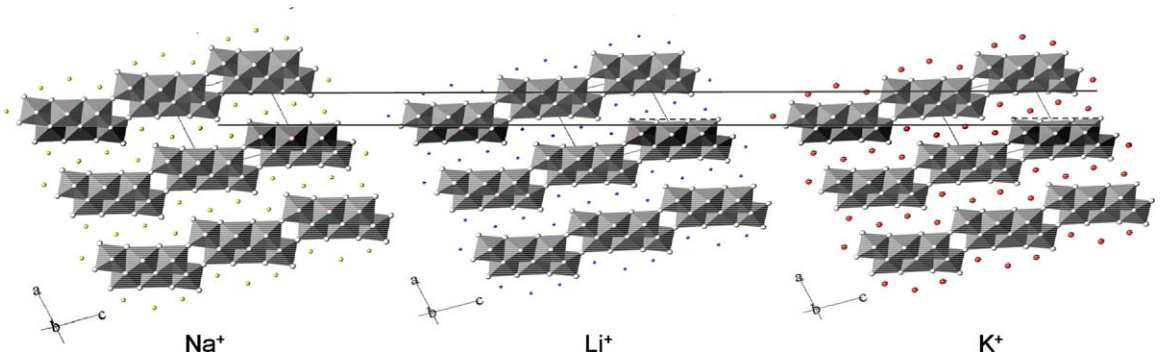

Fig. 4. Schematic figure showing decrease of the interlayer distance when Na^+ is replaced by Li^+ and K^+. Na^+, K^+ and Li^+ were represented by yellow, blue, and red circles, respectively. TiO_6^- units were represented by gray octahedra. The black lines are used to illustrate the different interplanar distances.

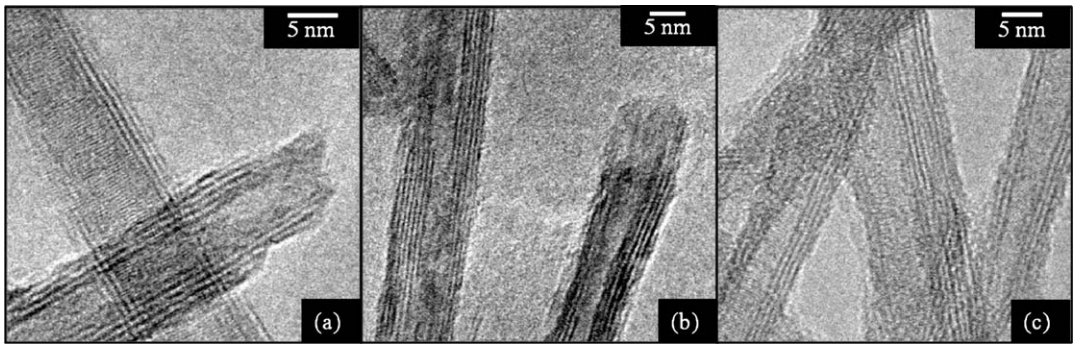

Fig. 5. High resolution TEM images of (a) K^+, (b) Li^+ and (c) Na^+ intercalated titanate nanotubes.

interlayer distance, as observed earlier [34], cannot be explained by dependence on ionic radii, because K^+ has the largest radius as compared with Li^+ and Na^+. The contraction of layers due to K^+ intercalation has also been observed for other titanates [34]. We do not have a model for explaining the interlayer contraction in case of K^+ intercalation but this phenomenon is also tracked in the low wavenumber Raman modes where K. . .O–Ti bending mode exhibits shift towards lower wavenumbers when Na^+ is replaced by K^+ (from 196 to 189 cm^{-1}, respectively) and thus indicating an increase of potassium–titanium distance in K. . .O–Ti (see Table 1).

Fig. 5, high resolution TEM images of (a) K^+, (b) Li^+ and (c) Na^+ intercalated titanate nanotubes, shows that tubular morphology was preserved as described in other works [6,20]. We also observed changes in the average interlayer distance being 0.73, 0.75 and 0.77 nm for K^+, Li^+ and Na^+ intercalated titanate nanotubes, respectively, the same sequence as those observed in X-ray data. The average interlayer distance in Na-TiNT was observed in previous studies between 0.8 and 0.9 nm, depending of the Na solution concentration in the synthesis of the titanate nanotubes [16,18,35]. The deviation between HRTEM observation and XRD detection may be caused by the dehydration of the titanate nanotube samples when they are exposed to the electron beam during HRTEM measurements.

EDS (energy dispersive X-ray spectroscopy) analyses were employed (see Supplementary Material) for evaluating the chemical composition after the K^+ ion exchange reactions. The EDS analyses showed an almost total exchange of Na^+ by K^+, but there is still some residual amount of Na^+ in the exchanged nanotubes.

4. Conclusions

Vibrational, structural and morphological properties of alkali–metal intercalated titanate nanotubes have been reported. We have confirmed that the tubular morphology and structure are preserved after promoting the ionic exchange reactions with Li^+ and K^+. Vibrational spectroscopy had shown that some vibrational modes were affected by the ionic exchange reactions. The most affected mode is that related to Ti–O bonds whose oxygen is not shared among the TiO_6 units (at the corner of the TiO_6 octahedral slabs) and its wavenumber increases as the ion electronegativity increases. The wavenumber dependence of Ti–O modes on different alkali intercalation provides evidences that the structure of titanate layers is similar to trititanate bulk structure. Additionally, this study shows that vibrational spectroscopy is very useful for probing metal intercalated titanate nanotubes.

Acknowledgements

Financial support from the Brazilian funding agencies CNPq, CAPES, FUNCAP, FAPEPI and FAPESP is gratefully acknowledged. The authors are indebted to Dr. Eduardo Padrón Hernández (CETENE, Brazil) for his assistance with the TEM measurements. This is a contribution from Institute of Science, Technology and Innovation on Functional Complex Materials (Inomat) and INCT NanoBioSimes. AGSF acknowledge support from CNPq grant 306335/2007-7. BCV, AGSF and AAI acknowledge the support from Projeto Casadinho CNPq 620238/2008-9.

Appendix A. Supplementary data

Supplementary data associated with this article can be found, in the online version, at doi:10.1016/j.vibspec.2010.11.007.

References

[1] A. Fujishima, K. Hashimoto, T. Watanabe, TiO_2 Photocatalysis. Fundamentals and Applications, BKC, USA, 1999.
[2] D.V. Bavykin, F.C. Walsh, Eur. J. Inorg. Chem. 2009 (2009) 977–997.
[3] X. Chen, S.S. Mao, Chem. Rev. 107 (2007) 2891–2959.
[4] V. Idakiev, Z.Y. Yuan, T. Tabakova, B.L. Su, Appl. Catal. A: Gen. 281 (2005) 149–155.
[5] R. Tenne, Nat. Nanotechnol. 1 (2006) 103–111.
[6] B.C. Viana, O.P. Ferreira, A.G. Souza Filho, C.M. Rodrigues, S.G. Moraes, J. Mendes, O.L. Alves, J. Phys. Chem. C 113 (2009) 20234–20239.
[7] S. Zhang, Q. Chen, L.M. Peng, Phys. Rev. B 71 (2005) 014104-1–114104-11.
[8] D. Fang, K. Huanh, S. Liu, J. Huang, J. Braz. Chem. Soc. 19 (2008) 1059–1064.
[9] T. Kasuga, M. Hiramatsu, A. Hoson, T. Sekino, K. Niihara, Adv. Mater. 11 (1999) 1307–1311.
[10] D.V. Bavykin, V.N. Parmon, A.A. Lapkin, F.C. Walsh, J. Mater. Chem. 14 (2004) 3370–3377.
[11] Y.Q. Wang, G.Q. Hu, X.F. Duan, H.L. Sun, Q.K. Xue, Chem. Phys. Lett. 365 (2002) 427–431.
[12] B.D. Yao, Y.F. Chan, X.Y. Zhang, W.F. Zhang, Z.Y. Yang, N. Wang, Appl. Phys. Lett. 82 (2003) 281–283.
[13] S. Zhang, L.M. Peng, Q. Chen, G.H. Du, G. Dawson, W.Z. Zhou, Phys. Rev. Lett. 91 (2003) 2561031–2561034.
[14] B.C. Viana, O.P. Ferreira, A.G. Souza Filho, J. Mendes Filho, O.L. Alves, J. Braz. Chem. Soc. 20 (2009) 167–175.
[15] Q. Chen, G.H. Du, S. Zhang, L.M. Peng, Acta Crystallogr. B 58 (2002) 587–593.
[16] X.M. Sun, Y.D. Li, Chem: A Eur. J. 9 (2003) 2229–2238.
[17] D. Wu, J. Liu, X.N. Zhao, A.D. Li, Y.F. Chen, N.B. Ming, Chem. Mater. 18 (2006) 547–553.
[18] O.P. Ferreira, A.G. Souza Filho, J. Mendes Filho, O.L. Alves, J. Braz. Chem. Soc. 17 (2006) 393–402.
[19] E. Morgado, B.A. Marinkovic, P.M. Jardim, M.A.S. de Abreu, F.C. Rizzo, J. Solid State Chem. 182 (2009) 172–181.
[20] J.Q. Huang, Y.G. Cao, Q.F. Huang, H. He, Y. Liu, W. Guo, M.C. Hong, Cryst. Growth Des. 9 (2009) 3632–3637.
[21] R.Z. Ma, K. Fukuda, T. Sasaki, M. Osada, Y. Bando, J. Phys. Chem. B 109 (2005) 6210–6214.
[22] D.J. Yang, Z.F. Zheng, H.Y. Zhu, H.W. Liu, X.P. Gao, Adv. Mater. 20 (2008) 2777–2781.
[23] X. Ding, X.G. Xu, Q. Chen, L.M. Peng, Nanotechnology 17 (2006) 5423–5427.
[24] J.Q. Geng, Z.Y. Hang, Y. Wang, D. Yang, Scripta Mater. 59 (2008) 352–355.
[25] L. Hongwei, Y. Dongjiang, R.W. Eric, K. Xuebin, Z. Zhanfeng, Z. Huaiyong, L.F. Ray, J. Raman. Spectrosc., in press.
[26] L. Hongwei, Y. Dongjiang, R.W. Eric, K. Xuebin, Z. Zhanfeng, Z. Huaiyong, L.F. Ray, J. Raman Spectrosc., in press.
[27] S. Andersson, A.D. Wadsley, Acta Crystallogr. 14 (1961) 1245–1249.

[28] S. Papp, L. Korosi, V. Meynen, P. Cool, E.F. Vansant, I. Dekany, J. Solid State Chem. 178 (2005) 1614–1619.
[29] L. Hongwei, Y. Dongjiang, R.W. Eric, K. Xuebin, Z. Zhanfeng, Z. Huaiyong, L.F. Ray, J. Raman Spectrosc. 41 (2010) 1331–1341.
[30] Y. Su, M.L. Balmer, B.C. Bunker, J. Phys. Chem. B 104 (2000) 8160–8169.
[31] X.Y. Liu, N.J. Coville, S. Afr. J. Chem. 58 (2005) 110–115.
[32] S. Pavasupree, Y. Suzuki, S. Yoshikawa, R.J. Kawahata, Solid State Chem. 178 (2005) 3110–3116.
[33] R.D. Shannon, C.T. Prewitt, Acta Crystallogr. B: Struct. B 25 (1969) 925–946.
[34] X.D. Wang, Z.S. Jin, X.R. Pei, J.J. Yang, Z.J. Zhang, Chin. Chem. Lett. 17 (2006) 1275–1278.
[35] K. Yoshida, L. Miao, N. Tanaka, S. Tanemura, Nanotechnology 20 (2009) 405709.